Influence of Re on the propagation of a Ni/Ni_3 Al interface crack by molecular dynamics simulation

2013 Modelling Simul. Mater. Sci. Eng. 21 045009

(http://iopscience.iop.org/0965-0393/21/4/045009)

Modelling Simul. Mater. Sci. Eng. **21** (2013) 045009 (14pp) doi:10.1088/0965-0393/21/4/045009

Influence of Re on the propagation of a Ni/Ni_3 Al interface crack by molecular dynamics simulation

Zheng-Guang Liu[1,4], **Chong-Yu Wang**[1,2,3] **and Tao Yu**[1]

[1] Central Iron and Steel Research Institute, Beijing 100081, People's Republic of China
[2] Department of Physics, Tsinghua University, Beijing 100084, People's Republic of China
[3] International Centre for Materials Physics, Academia Sinica, Shenyang 110016, People's Republic of China
[4] Department of Physics, North University of China, Taiyuan 030051, People's Republic of China

E-mail: cywang@mail.tsinghua.edu.cn

Received 2 November 2012, in final form 27 February 2013
Published 12 April 2013
Online at stacks.iop.org/MSMSE/21/045009

Abstract

The influence of Re on the propagation of a (0 1 0)[1 0 1] crack in the Ni/Ni_3Al interface, including crack propagation velocity, crack-tip shape, and dislocation emission, is investigated using a molecular dynamics method with a Ni–Al–Re embedded-atom-method potential. The propagation velocity of the crack noticeably decreases at 5 K when 3 or 6 at% Re atoms are added into the Ni matrix. At 1033 K, the crack tip becomes blunter and emission of dislocations becomes easier with Re addition, owing to the larger bond strength between Re and Ni atoms. Furthermore, we calculate the unstable stacking energy (γ_{us}), surface energy (γ_s), and adhesion work (W_{ad}) of the interface. When Re atoms are randomly doped into a Ni matrix, γ_s/γ_{us} increases correspondingly. This means that Re addition decreases brittleness and improves ductility. The calculation also shows that γ_{us} is not affected by Re–Ni atomic interaction, and that Re–Re atomic interaction has some effect on γ_{us}. In addition, W_{ad} increases with Re addition, and a small increase in W_{ad} results in a larger decrease in crack velocity. This indicates that Re–Ni atomic interaction restrains crack propagation velocity at low temperature.

(Some figures may appear in colour only in the online journal)

1. Introduction

Ni-based single-crystal superalloys have excellent strength at high temperatures, and have been used in turbine blades in aeroengines [1, 2]. These superalloys consist of a Ni-based matrix (fcc γ phase) with a dispersion strengthening phase, i.e., the ordered intermetallic precipitate

particles of Ni_3Al (L12 γ' phase). Rhenium is a crucial element in Ni-base single-crystal superalloys, and creep rupture and fatigue strength can be markedly improved by the addition of Re [3–5]. The generation of Ni-based single-crystal superalloys is closely related to their Re concentration. 0, 2–4 and 5–7 wt% Re are included in the compositions of the first, second and third generation Ni-base superalloys [6, 7], respectively. The increase of strength (including creep rupture and fatigue strength) with Re addition is often attributed to retardation of the diffusional coarsening of γ' precipitates [8] and difficult climbing of dislocations in the γ/γ' interface [6].

In macroscopic experiments, the position and construction of atomistic cracks are difficult to ascertain. The topologically closed-packed (TCP) phase is regarded as the cradle of cracks in these superalloys, whereas TCP phases can be constrained through the addition of Ru [9]. The intersection of deformation twin plates with the specimen surface is considered to be a cause of microcracking in thermomechanical fatigue (TMF) experiments, and the propagation of a crack along the twin boundaries can lead to TMF failure of the specimen [10]. From a more microscopic viewpoint, some experiments on fatigue cracking have demonstrated that cracks often propagate along the γ/γ' interface or in the γ phase [11–13].

On the atomic scale, the final rupture is caused by the breaking of atomic bonds, and crack propagation and movement of dislocations should be taken into account. The rupture strength is likely to be improved by stronger atomic bonding between solute and matrix atoms during the propagation of atomistic cracks. Therefore, it is necessary to study the influence of Re on the propagation of γ/γ' (Ni/Ni_3Al) interface cracks.

Temperature is also an important factor in rupture strength because cracks often propagate in a brittle manner at low temperature and in a ductile manner at high temperature in superalloys. In practice, the root and tip parts of a turbine blade work at low and high temperature, respectively, and the influence of Re on crack propagation can change with temperature. The crack propagation path may be altered at different temperatures, especially after alloying elements are doped into superalloys. Therefore, the effect of temperature on crack propagation must also be considered. Although the Ni-based single-crystal superalloys often work at between 600 ° and 1000 ° during service under stress, the crack propagation at 5 K is also explored in the present work to analyze the mechanism of brittle fracture.

There is a lack of literature on the mechanisms of γ/γ' interface dynamic rupture on the atomic level. Only a few studies with molecular dynamics (MD) simulations and *ab initio* calculations have been completed for Ni, Ni_3Al, NiAl and Ni/Ni_3Al interfaces. Using the MD method, Hess *et al* [14] studied the competition between crack growth and dislocation emission for a crack tip in Ni, and pointed out that temperature and crystal orientation have an important influence on the process of dislocation nucleation. Xie *et al* [15, 16] explored the process of atomic configuration evolution and deformation behavior at a crack tip in Ni_3Al using MD, and showed that pseudo-twins are formed on {1 1 1} planes in the crack-tip zone. Guo *et al* [17] studied the mechanisms of low-temperature deformation at a crack tip in B2 NiAl by MD simulation, and found that stress induced martensitic transformation occurs at the crack tip. Using density functional theory (DFT) and in terms of Griffith work, Gong *et al* [18] investigated strengthening effects induced by alloying elements on an Ni/Ni_3Al interface, and showed clearly that the best strengthening element is Re. Chen *et al* [19] calculated the bond orders of a Ni/Ni_3Al interface doped with alloying elements using the first-principles Dmol3 package, and found that the cohesive strength of the interface can be improved by Mo, W, Re and Ta. However, in these *ab initio* studies, dynamic evolution of the crack and temperature effects were not considered.

In the present work, the influence of Re on the propagation of a Ni/Ni_3Al interface crack, including on crack propagation velocity, crack-tip shape, and the emission of dislocations is

investigated using an MD method with a Ni–Al–Re embedded-atom-method (EAM) potential [20]. This potential provides an accurate fit to the lattice parameter, cohesive energy, vacancy formation energy and elastic constants of Ni, Al and Re, and their compounds. MD simulations are carried out at 5 K and 1033 K, respectively. Furthermore, some quantities, including the ratio of surface energy to unstable stacking energy in the Ni matrix, and the adhesion work on the interface, are calculated to evaluate the effect of Re on dislocation emission and crack propagation velocity.

The present work is organized as follows. The model and procedures for the MD simulation of an interface crack are described in section 2. Section 3 contains the results and discussion for the MD simulations of a Ni/Ni_3Al interface crack doped with Re. Finally, the conclusions are summarized in section 4.

2. Model and procedures

In the present work, an atomistic sharp crack in the Ni/Ni_3Al interface is initially constructed by the anisotropic elastic displacement field [21]. A coherent interface is used. As shown in figure 1(*a*), the crack is oriented at $x = [1\,0\,\bar{1}]$, $y = [0\,1\,0]$ and $z = [1\,0\,1]$. The crack surface is a (0 1 0) plane, and the crack front is oriented along the [1 0 1] direction. The simulated system, in which the upper half is Ni_3Al and the lower half is Ni, consists of 132 atomic layers along the $x[1\,0\,\bar{1}]$ direction, 138 atomic layers along the $y[0\,1\,0]$ direction and 16 atomic layers along the $z[1\,0\,1]$ direction, to include a total of 72864 atoms. A larger system (276 atomic layers along the $y[0\,1\,0]$ direction) has been used, and it was found that the crack propagation velocity and configuration evolution on the crack tip are insensitive to system size. The initial crack length is about $l = 40$ Å.

Two kinds of Ni/Ni_3Al interface cracks are constructed according to the joint mode between Ni and Ni_3Al (figures 1(*b*) and (*c*)). In figure 1(*b*), both the upper and lower surfaces of the crack consist of Ni atoms and no Al atoms; in figure 1(*c*), the lower surface of crack consist of Ni atoms, and the upper surface of crack consist of Ni and Al atoms. In the present MD simulation, when the crack propagates along the Ni/Ni_3Al interface, the surfaces of crack are found to follow that in figure 1(*b*), although the initial crack is constructed in figure 1(*c*). Thus, the mode of interface crack in figure 1(*b*) is adopted in the present work.

In practice, the γ/γ'(Ni/Ni_3Al) interface in Ni-based single-crystal superalloy is a diffuse interface between γ/γ' phases of which the width is about 1–3 nm [22, 23]. In the literature [23], the study revealed the presence of two interfacial widths, one corresponding to an order–disorder transition, and the other to the compositional transition across the interface, raising fundamental questions regarding the definition of the interfacial width in such systems. In addition, the structure optimization of the interface model with transition layers is also a problem due to the coexistence for many interface structures. Therefore, the interface model with transition layers is constructed difficultly and not adopted in the present work.

The elasticity theory of interface cracking was proved to be applicable in the macroscopic fracture mechanics by Rice [24], and the anisotropic elastic theory of interface cracking has also been given by Suo [21]. To simplify the MD simulation and use anisotropic elastic theory, we adopted an interface model without transition layers, and found that the propagation path of brittle cracks does not vary with the atomic concentration of Re near the interface at low temperature. At higher temperature, the crack often propagates in a ductile manner and transition layers may then have some effect on the emission of dislocations near the crack tip, with the result that the effect of alloying elements on the emission of dislocations near the crack tip cannot be easily determined. Thus, an interface model without transition layers is adopted in the present work.

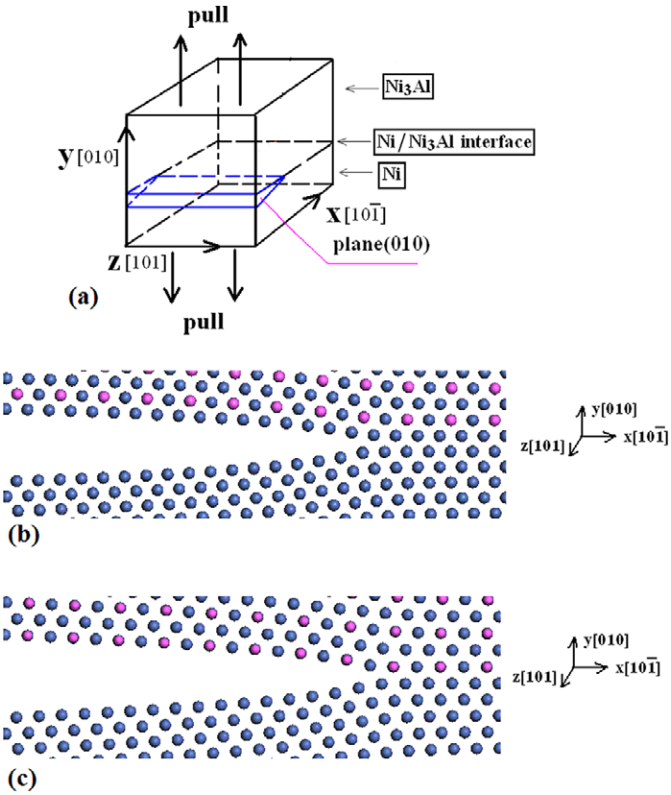

Figure 1. (*a*) Structural model of the Ni/Ni_3Al interface crack (blue lines); (*b*) Ni–Ni joint interface crack, and both the upper and lower surfaces of crack consist of Ni atoms and no Al atoms; (*c*) Al–Ni joint interface crack, and the lower surface of crack consists of Ni atoms, and the upper surface of crack consists of Ni and Al atoms.

The crack system is first relaxed (for 5 ps) to equilibrium. Then, to find out the dynamic velocity of the crack, the crack system is loaded in mode I, i.e., strain loading in the $y[0\,1\,0]$ direction is carried out. Strain rate $\dot{\varepsilon} = 1 \times 10^9\,\mathrm{s}^{-1}$ is used. Fixed boundary conditions (the outermost 4 layers of atoms are fixed) are used in both $x[1\,0\,\bar{1}]$ and $y[0\,1\,0]$ directions. The periodic boundary condition is used in the $z[1\,0\,1]$ direction. Newton's equations of motion in MD are solved by the Gear algorithm [25]. Time steps of 5×10^{-15} s and 1×10^{-15} s are used at 5 K and 1033 K, respectively. The temperature of the system remains invariant throughout the simulation, obtained by scaling the instantaneous velocities of all atoms with the appropriate Maxwell–Boltzmann distribution at a specified temperature. The XMD program [26] is used for the atomistic simulations.

Because the Re atoms tend to distribute randomly in the γ phase and are not prone to clustering in nickel-based single crystal superalloys [22, 27], 3 or 6 at% Re is randomly doped into the Ni matrix in the present MD simulation. These atomic concentrations are in the range of those used experimentally [28]. In addition, when 3 at% Re was doped into Ni_3Al, it was found that an interface crack still advanced along the interface or into the Ni matrix, which indicated that Re doping has no effect on the propagation path of an interface crack in Ni_3Al. Consequently, in the present work Re is only doped into the Ni matrix to study its influence on the propagation of an interface crack.

3. Results and discussion

3.1. Influence of Re on the bluntness of crack tip and the emission of dislocation

In order to probe the influence of Re on crack-tip bluntness, the variation of crack-tip shape and dislocations near the crack tip are observed in the MD simulation. Figure 2 shows variation of the crack-tip shape at 20 ps under strain rate $\dot{\varepsilon} = 1 \times 10^9\ \mathrm{s}^{-1}$ at 5 K with Re addition (0, 3 or 6 at%). It can be seen from figures 2(*a*)–(*c*) that at low temperature (5 K), the crack propagates along the interface in a cleavage manner, and the crack tip remains atomically sharp even when at a Re concentration of 6 at%. In the meantime, dislocations do not appear around the crack tip. It is also seen from figure 2 that the crack path is not changed by the addition of 3 or 6 at% Re.

Figure 3 shows variation of the crack-tip shape at 20 ps under strain rate $\dot{\varepsilon} = 1 \times 10^9\ \mathrm{s}^{-1}$ at 1033 K with Re addition (0, 3 and 6 at%). From figures 3(*a*)–(*c*), it can be seen that at 1033 K the crack tip becomes blunt and the crack propagates in a ductile manner in the Ni matrix. Thus, temperature has an obvious effect on ductility.

The above MD simulations show that the crack propagates in the Ni matrix or Ni/Ni_3Al interface, not in the Ni_3Al. This is consistent with the results of fatigue experiments for low stress [11].

It can also be seen from figure 3 that with increasing atomic concentration of Re, the crack tip becomes blunter and the curvature radius of the crack tip rises. The crack tip tends to be more blunt with Re addition due to the high bond strength between Re and Ni atoms; the Re–Ni interatomic interaction is stronger than that of Ni–Ni. The high atomic interaction of Re–Ni can prevent the breaking of atomic bonds in the cleavage plane. Due to the competition between cleavage and dislocation emission, dislocation emission near the crack tip becomes easier because it becomes more difficult to break the atomic bonds, and the crack tip becomes more blunt as a result. However, without the addition of Re, atomic bond breaking takes place more easily and the crack tip becomes sharper. In order to analyze the competition between cleavage and dislocation emission, the surface energy and unstable stacking energy in the Ni matrix are calculated in the following sections.

Figure 4 shows the variation of pair potential with the distance between two Ni–Ni or Ni–Re atoms. The pair-potential part of the EAM total energy for Ni is obtained in fcc structure; the pair-potential part of the EAM total energy for Ni–Re atoms is obtained in $L1_2$-Ni_3Re, $D0_{19}$-Ni_3Re, $D0_{22}$-Ni_3Re, B_2-NiRe and $L2_1$-Ni_2ReAl structures [20]. In these structures, the volumes are relaxed to equilibrium, and the lattice constants and the binding energies of the structures are fitted according to the experiments or first-principles data. It can be seen from figure 4 that the depth of the potential well for Ni–Re is much larger than that of Ni–Ni, indicating that it is more difficult to break Ni–Re atomic bonds.

The level of atomic bond breaking near a crack tip can be estimated by the following expression

$$P(t) = \sum_{i=1}^{n} P_i(t)/n, \tag{1}$$

where $P_i(t)$ is the first-neighbor number of atom i situated in the crack-tip zone at moment t and n is the number of atoms in the crack-tip zone, here $n = 581$. Table 1 lists $P(t)$ at 0, 10 and 20 ps for Re addition of 0, 3 and 6 at% under strain rate $\dot{\varepsilon} = 1 \times 10^9\ \mathrm{s}^{-1}$ at 1033 K. In table 1, the concentrations of Re atoms in the crack-tip zone are 2.4 and 4.3, not 3 and 6 at%, due to the scheme having random doping of Re atoms in the Ni matrix. In table 1, the calculated value of $P(t)$ for the total 581 atoms rises with Re concentration (except 3 at% Re at

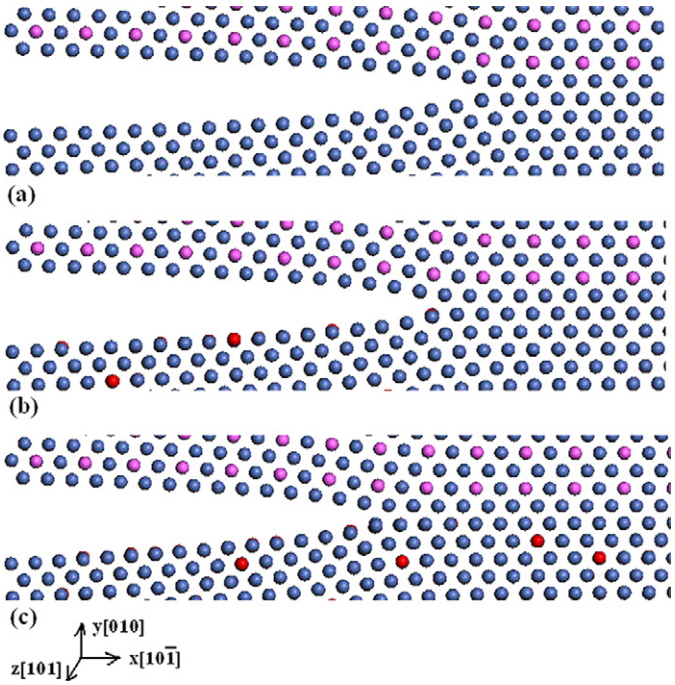

Figure 2. Variation of crack-tip shape at 20 ps under strain rate $\dot{\varepsilon} = 1 \times 10^9\ \mathrm{s}^{-1}$ at 5 K. Blue, pink and red balls represent Ni, Al and Re atoms, respectively. (*a*) Without Re addition; (*b*) with 3 at% Re; (*c*) with 6 at% Re.

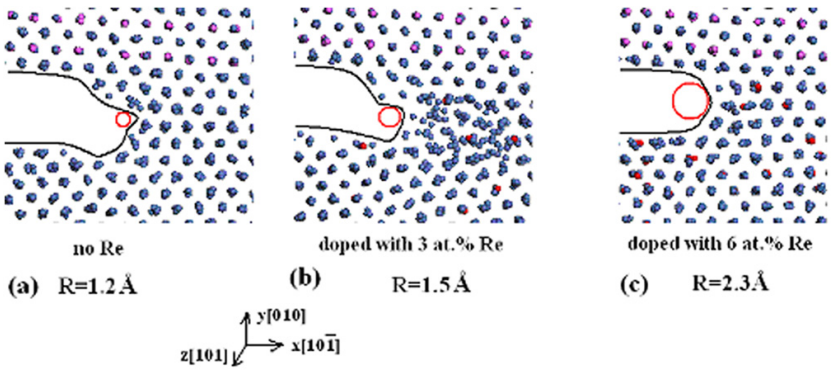

Figure 3. Variation of crack-tip shape with atomic concentration of Re at 20 ps under strain rate $\dot{\varepsilon} = 1 \times 10^9\ \mathrm{s}^{-1}$ at 1033 K. Red circles represent the circle of curvature at the crack tips. Blue, pink and red balls represent Ni, Al, and Re atoms, respectively. Crack-tip curvature radius (*a*) without Re addition ($R = 1.2$ Å) ; (*b*) with 3 at% Re ($R = 1.5$ Å); (*c*) with 6 at% Re ($R = 2.3$ Å).

20 ps), and the values of $P(t)$ calculated for Re atoms are larger than those for Ni atoms. This shows that the first-neighbor number of Re atoms is larger than that of Ni atoms, implying a stronger cohesiveness Re–Ni atoms than Ni–Ni atoms and that the level of atomic bond breaking drops with Re addition. Herein, the value of $P(t)$ calculated for Al atoms is only listed and not discussed because the interface crack does not propagate within Ni_3Al in the MD simulation.

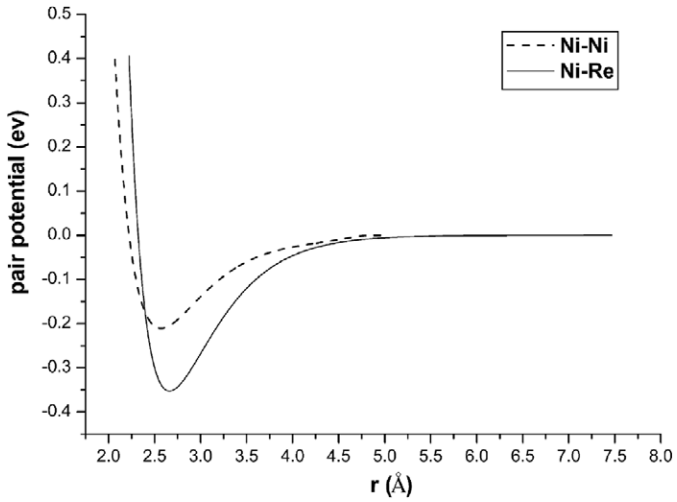

Figure 4. Variation of pair potential with distance between two Ni–Ni or Ni–Re atoms.

Table 1. Calculated $P(t)$ at moment t under strain rate $\dot{\varepsilon} = 1 \times 10^9\,\mathrm{s}^{-1}$ at 1033 K.

		$t = 0$ ps	$t = 10$ ps	$t = 20$ ps
$P(t)$ (0 at% Re)	Total atoms ($n = 581$)	9.82	9.56	9.37
	Al atoms ($n = 28$)	6.96	7.15	7.22
	Ni atoms ($n = 553$)	9.96	9.68	9.47
$P(t)$ (3 at% Re)	Total atoms ($n = 581$)	9.85	9.58	9.26
	Re atoms ($n = 14$)	10.21	10.57	10.14
	Al atoms ($n = 28$)	7.09	7.03	7.09
	Ni atoms ($n = 539$)	10.00	9.70	9.36
$P(t)$ (6 at% Re)	Total atoms ($n = 581$)	9.96	10.00	9.84
	Re atoms ($n = 25$)	10.44	10.68	10.68
	Al atoms ($n = 28$)	7.46	7.64	7.64
	Ni atoms ($n = 528$)	10.06	10.09	9.91

Emission of dislocations is observed under strain rate $\dot{\varepsilon} = 1 \times 10^9\,\mathrm{s}^{-1}$ at 1033 K in the present MD simulation when 0, 3, or 6 at% Re is doped into the Ni matrix. We have found that dislocations near the crack tip do not appear before 10 ps with the addition of 0 or 3 at% Re, and that some dislocations are emitted from the crack tip before 10 ps when the Re concentration is 6 at%. This means that the emission of dislocations becomes easier and the crack tip becomes more blunt when the atomic concentration of Re is raised to 6 at%. The dislocation configurations near the crack tip at 10 ps under strain rate $\dot{\varepsilon} = 1 \times 10^9\,\mathrm{s}^{-1}$ for 6 at% Re are depicted in figure 5. $a/6 < 1\,1\,2 > \{1\,1\,1\}$ partial dislocations appear in atomic layers 1, 2, 3, 4 and 5 near the crack tip (parameter a is the lattice constant). From figure 5(*a*), it is seen that atomic layers 1, 3 and 4 slip relative to atomic layers 2, 4 and 5 in the $\{1\,1\,1\}$ plane, and the crack tip becomes blunt. From figure 5(*b*), atomic layer 1 slips relative to atomic layer 2 (atomic layer 1 is the outer layer perpendicular to the $(\bar{1}\,1\,1)$ plane), and an $a/6[1\,\bar{1}\,2](\bar{1}\,1\,1)$ partial dislocation appears between them. This results in atomic layer 1 slipping far from the crack tip. From figure 5(*c*), atomic layer 3 slips relative to atomic layer 4 (atomic layer 4 is the outer layer perpendicular to the $(1\,1\,\bar{1})$ plane), and an $a/6[\bar{2}\,1\,\bar{1}](1\,1\,\bar{1})$

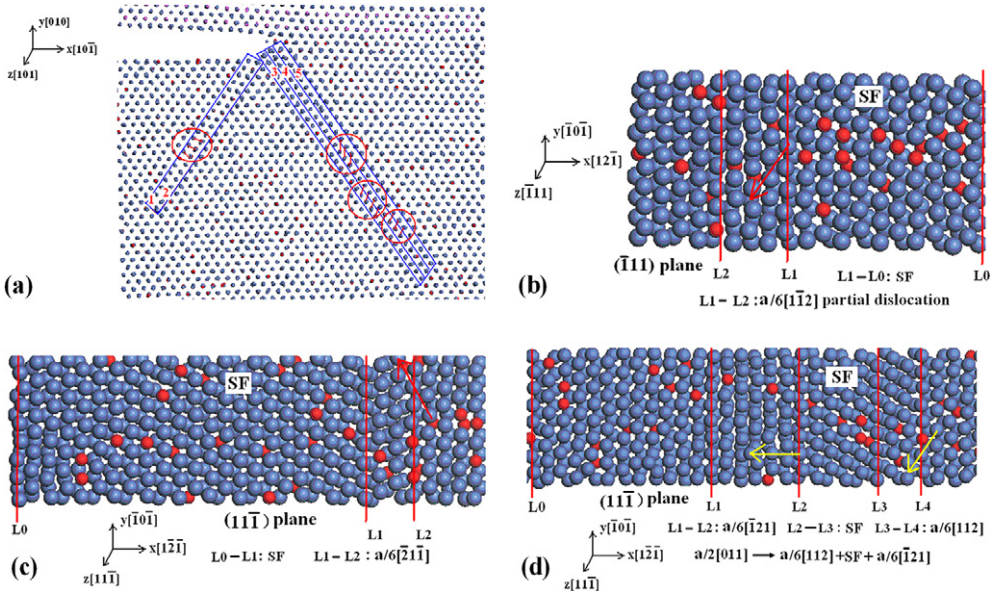

Figure 5. Atomic configurations of the crack tip and corresponding dislocations at 10 ps under strain rate $\dot{\varepsilon} = 1 \times 10^9\ \mathrm{s}^{-1}$ for 6 at% Re at 1033 K. Blue, pink and red balls represent Ni, Al and Re atoms, respectively. SF represents the stacking fault in the $\{1\,1\,1\}$ plane. L_0 is the position of the crack tip. (*a*) $a/6 < 1\,1\,2 > \{1\,1\,1\}$ partial dislocations in atomic layers 1, 2, 3, 4 and near the crack tip; (*b*) $a/6[1\,\bar{1}\,2](\bar{1}\,1\,1)$ partial dislocation between atomic layers 1 and 2; (*c*) $a/6[\bar{2}\,1\,\bar{1}](1\,1\,\bar{1})$ partial dislocation between atomic layers 3 and 4; (*d*) $a/2[0\,1\,1](1\,1\,\bar{1})$ extended dislocation between atomic layers 4 and 5.

partial dislocation appears between them, which results in atomic layer 3 slipping far from the crack tip. From figure 5(*d*), atomic layer 4 slips relative to atomic layer 5 (atomic layer 5 is the outer layer perpendicular to the $(1\,1\,\bar{1})$ plane), and an $a/2[0\,1\,1](1\,1\,\bar{1})$ extended dislocation appears between them, which results in the atomic layer 4 slipping far from the crack tip. The $a/2[0\,1\,1](1\,1\,\bar{1})$ extended dislocation equation in the $(1\,1\,\bar{1})$ plane.

$$a/2[0\,1\,1] \rightarrow a/6[1\,1\,2] + SF + a/6[\bar{1}\,2\,1]. \tag{2}$$

This dislocation reaction can be often found in the Ni matrix and has been confirmed by electron microscopy [29].

3.2. Influence of Re on the surface energy and the unstable stacking energy

The competition between cleavage and dislocation emission can be evaluated by the ratio of the surface energy to the unstable stacking energy [30]. Although this ratio does not often accurately predict the critical stress intensity factor for dislocation emission in atomistic simulations, the trend of competition between cleavage and dislocation emission with Re addition can be obtained. The surface energy (γ_s) of the $(1\,0\,0)$ plane and the unstable stacking energy (γ_{us}) of the $a/6 < 1\,1\,2 >$ Shockley partial dislocation were calculated using the MD method and are listed in tables 2 and 3, respectively.

The calculation of γ_s of the $(1\,0\,0)$ plane is carried out for the Ni matrix since both the upper and lower surfaces of crack consist of Ni atoms and no Al atoms (figure 1(*b*)). The computational model for γ_s consists of 8000 atoms, with 20 atomic layers along the $x[0\,0\,1]$

Table 2. Values of γ_s from the MD calculation.

Re concentration	0 at%	3 at%	6 at%
γ_s (J m^{-2})	1.5915	1.6127	1.6538

Table 3. Values of γ_{us} from the MD calculation. Mode I is constructed without Re addition; in mode II, 6 at% Re is placed in the lower atomic layer across the slip plane; in mode III, 6 at% Re is placed in both the lower and upper atomic layers across the slip plane. The Re atoms are reciprocally the first nearest neighbor; in mode IV, 6 at% Re is randomly placed in both the lower and upper atomic layers across the slip plane.

	Mode I	Mode II	Mode III	Mode IV
γ_{us} (J m^{-2})	0.2775	0.2768	0.2548	0.2746

direction, 40 atomic layers along the $y[1\,0\,0]$ direction and 20 atomic layers along the $z[0\,1\,0]$ direction. γ_s can be obtained in the following equation

$$\gamma_s = (E_2 - E_1)/(2S_{(1\,0\,0)}), \tag{3}$$

where E_2 is the potential energy of the model when the periodic boundary condition is used in the x and z directions, and the y direction is taken as a free surface, E_1 is the potential energy of the model when the periodic boundary condition is used in the x, z and y directions, and $S_{(1\,0\,0)}$ is the area of the (1 0 0) plane.

Compared with the surface energy of pure Ni matrix, the surface energy of the (1 0 0) plane increases by 1.3% and 3.9% with the addition of 3 at% and 6 at% Re, respectively (table 2).

The value of γ_{us}, which was introduced by Rice [30], can roughly evaluate the energy barrier of dislocation nucleation. In the present work, the calculation of γ_{us} of the $a/6[\bar{1}\,\bar{1}\,2]$ Shockley partial dislocation is carried out for the Ni matrix since the $a/6 < 1\,1\,2 >$ Shockley partial dislocations appear in the Ni matrix in the present MD simulation. The computational model for γ_{us} consists of 7200 atoms, with 36 atomic layers along the $x[1\,1\,2]$ direction, 60 atomic layers along the $y[1\,1\,\bar{1}]$ direction, and 20 atomic layers along the $z[\bar{1}\,1\,0]$ direction. The periodic boundary condition is used in the x and z directions, and the y direction is taken as a free surface. To calculate γ_{us}, the model is divided into two parts by the $(1\,1\,\bar{1})$ plane; the upper half is fixed while the lower half is slipped along the $[\bar{1}\,\bar{1}\,2]$ direction in the $(1\,1\,\bar{1})$ slip plane. During this slipping process in the $(1\,1\,\bar{1})$ plane, the system is allowed to relax in the y direction, and the relative energy difference of the model before and after the slip is calculated as [15]

$$E_{POT}(R, 0) = (E_{POT}(R) - E_{POT}(0))/S, \tag{4}$$

where R is the relative shear slip distance between the lower and upper parts, and $E_{POT}(R)$ and $E_{POT}(0)$ are the potential energies of the model at the relative slip distance R and 0, respectively. S is the total area of the $(1\,1\,\bar{1})$ plane. The value of γ_{us} can be roughly obtained when $R = 0.5b$, where b is the magnitude of the Burgers vector of the $a/6[\bar{1}\,\bar{1}\,2]$ Shockley partial dislocation.

For the calculation of γ_{us}, four modes are constructed according to the possible Re sites near the $(1\,1\,\bar{1})$ slip plane (shown in figure 6). Mode I (figure 6(a)) is constructed for the pure Ni without addition of Re. Mode II (figure 6(b)) is constructed considering the interaction between Re and Ni atoms. In mode II, 6 at% Re is placed in the lower atomic layer across the $(1\,1\,\bar{1})$ slip plane. Mode III (figure 6(c)) is constructed considering the interaction between Re and Re atoms. In mode III, 6 at% Re is placed in both the lower and upper atomic layers across the $(1\,1\,\bar{1})$ slip plane. The Re atoms are reciprocally the first nearest neighbor, and the

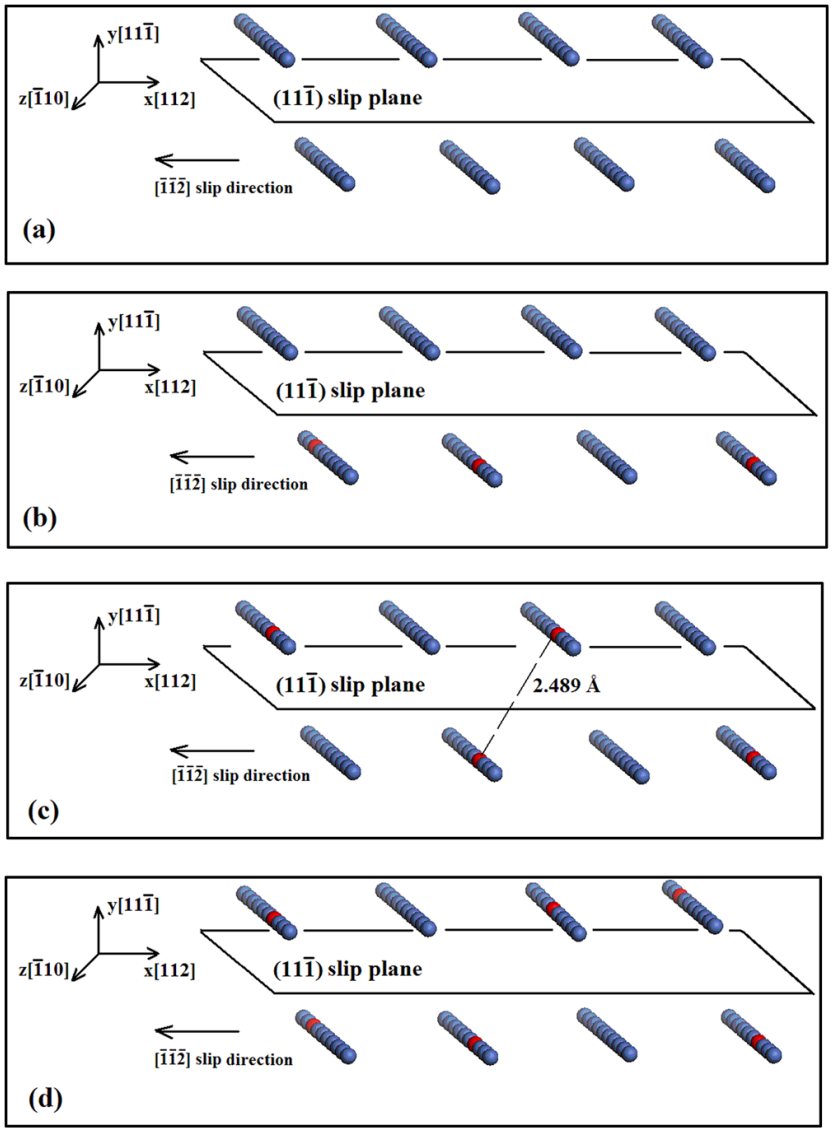

Figure 6. Re atom sites in the lower and upper atomic layers across the (1 1 $\bar{1}$) slip plane in the calculation model for γ_{us}. Blue and red balls represent Ni and Re atoms, respectively. (*a*) the pure Ni without addition of Re; (*b*) 6 at% Re is placed in the lower atomic layer across the slip plane; (*c*) 6 at% Re is placed in both the lower and upper atomic layers across the slip plane. The Re atoms are reciprocally the first nearest neighbor, and the distance between Re atoms is 2.489 Å before slip; (*d*) 6 at% Re is randomly placed in both the lower and upper atomic layers across the slip plane.

distance between Re atoms is 2.489 Å before slip, then increases during the slipping process. In mode IV (figure 6(*d*)), 6 at% Re is randomly placed in both the lower and upper atomic layers across the (11$\bar{1}$) slip plane.

As shown in table 3, γ_{us} decreases by 8.18% in mode III compared with mode I when 6 at% Re atoms are placed in both the lower and upper atomic layers across the (1 1 $\bar{1}$) slip

Table 4. Crack velocities ($m\,s^{-1}$) under strain rate $\dot{\varepsilon} = 1 \times 10^9 s^{-1}$ at 5 K.

	0 at% Re	3 at% Re	6 at% Re
Crack velocity (at 20 ps)	30	26	20
Crack velocity (at 45 ps)	70	40	30
Crack velocity (at 70 ps)	181	110	60

plane. Little variation of γ_{us} is found in mode II, in contrast with mode I, when the Re sites are only placed in the lower atomic layer across the slip plane. This means that the value of γ_{us} cannot be changed much by the interaction between Re and Ni atoms, but can be slightly decreased by interaction between Re atoms. In some reports [31, 32], the value of γ_{us} has been calculated by only taking interactions between the solute atoms and matrix atoms into account. However, the value of γ_{us} can be changed much more by solute–solute interaction [33]. In mode IV, γ_{us} changes little when 6 at% Re is randomly doped into Ni matrix. This means that γ_{us} cannot be greatly changed by Re from a statistical point of view in a solid solution, although the solute–solute interaction has been considered.

As a result, γ_s/γ_{us} slightly increases (by 5%) with random addition of 6 at% Re, compared with the pure Ni matrix, as can be seen from tables 2 and 3. This means that dislocations more easily appear and cleavage takes place with more difficulty when Re is randomly doped into the Ni matrix. As is seen from figure 5, dislocations more easily appear with the addition of 6 at% Re.

3.3. Influence of Re on the propagation velocity of crack

Using the MD method, the influence of Re on the propagation velocity of a brittle crack can be evaluated when 3 or 6 at% of atoms in the Ni matrix are randomly replaced by Re atoms. Table 4 lists values of crack velocity calculated under strain rate $\dot{\varepsilon} = 1 \times 10^9\ s^{-1}$ at 5 K, without and with Re addition. Only crack velocities before 70 ps are obtained in the MD simulation due to system size limits. From table 4, crack velocity obviously decreases with addition of 3 and 6 at% Re compared with that calculated without Re addition. At 1033 K, the crack propagates in a ductile manner and does not go forward, regardless of Re addition.

The reason for the decrease of the brittle crack velocity with Re addition at low temperature is very likely to be an increase of interatomic bond strength, because the Ni–Re bond is stronger than that of Ni–Ni. The interatomic bond strength can be reflected by the adhesion work, which is discussed in section 3.4.

3.4. Influence of Re on the adhesion work of interface

In this section, to investigate the reason for the observed change of crack propagation velocity with Re addition, the adhesion work (W_{ad}) of the Ni/Ni_3Al interface is calculated by the present MD method. The adhesion work is the reversible free-energy change for making free surfaces from interfaces [34]. During interfacial separation, atomic bonds near the crack tip are broken and crack surfaces are produced. The formation of these crack surfaces in unit time is related to the crack velocity. Thus, the brittle crack velocity may be in inverse proportion to the adhesion work.

Figure 7 shows the computational model for W_{ad} of the Ni/Ni_3Al interface. The computational model for W_{ad} consists of 5760 atoms, with 24 atomic layers along the $x[10\bar{1}]$ direction, 40 atomic layers along the $y[0\,1\,0]$ direction, and 24 atomic layers along the $z[1\,0\,1]$ direction. The periodic boundary condition is used in the x and z directions, and the y direction

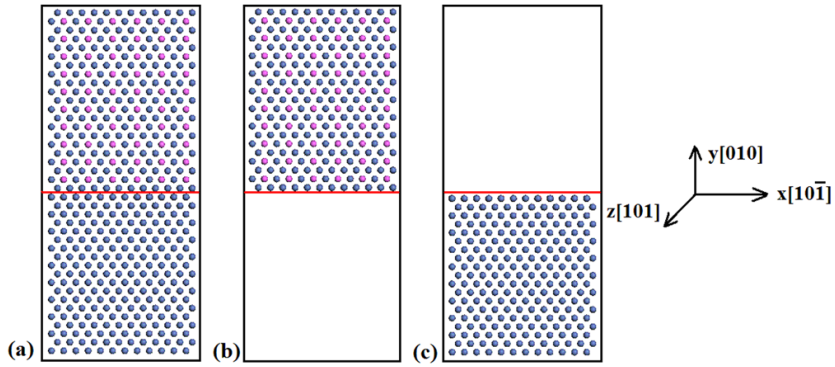

Figure 7. The computational model for W_{ad} of the Ni/Ni_3Al interface. The blue and pink balls represent Ni and Al atoms, respectively. The red line represents the interface. (*a*) Ni/Ni_3Al interface system; (*b*) Ni_3Al bulk; (*c*) Ni bulk.

Table 5. The adhesion work W_{ad} of interface at different Re concentration.

Re concentration	0 at%	3 at%	6 at%
W_{ad} (J m^{-2})	3.024	3.076	3.135

is taken as a free surface. The adhesion work W_{ad} of an interface can be easily determined using the following equation [35]:

$$W_{ad} = (E_A + E_B - E_{A/B})/S, \tag{5}$$

where $E_{A/B}$ is the total energy of a fully relaxed Ni/Ni_3Al interface system (shown in figure 7(*a*)). E_A and E_B are the energy of a fully relaxed slab Ni_3Al (shown in figure 7(*b*)) and slab Ni (shown in figure 7(*c*)), respectively. S is the interfacial area between slab Ni_3Al and slab Ni.

In the MD calculation of W_{ad}, 3 or 6 at% of atoms in the interface are uniformly replaced by Re atoms. The calculated values of W_{ad} are listed in table 5 and show that, compared with that obtained without Re addition, W_{ad} increases by 1.7% and 3.7% with the addition of 3 at% and 6 at% Re, respectively. Meanwhile, we notice that the brittle crack velocity decreases with Re addition even though the atomic concentration of Re is low (3 or 6 at%), as can be seen from table 4. Thus, a small variation of W_{ad} can result in a large change in crack velocity. The velocity of brittle cracking is in inverse proportion to the adhesion work. Furthermore, we predict that alloying elements with larger W_{ad} will hinder the propagation of brittle cracks, and this will be our future work.

4. Conclusions

In the present work, the influence of Re on the propagation of a Ni/Ni_3Al interface crack, including crack velocity, the shape of crack-tip shape, and dislocation emission, is investigated using a molecular dynamics method with a Ni–Al–Re EAM potential. The following conclusions have been drawn.

(1) The MD simulations show that at 5 K, the crack propagates along the interface in a cleavage manner, while at 1033 K the crack propagates in a ductile manner in Ni matrix, and not in the Ni_3Al. The trend of the crack path is consistent with fatigue experiments [11, 13].

In addition, at 1033 K the crack tip becomes blunt, and a $a/6 < 1\,1\,2 > \{1\,1\,1\}$ partial dislocation and $a/2[0\,1\,1](1\,1\,\bar{1})$ extended dislocation emitted from the crack tip appear in the Ni matrix, which has previously been confirmed by electron microscopy.

(2) At 1033 K, the crack tip becomes more blunt with Re addition due to the larger bond strength between Re and Ni atoms. Re–Ni atomic interaction can prevent breaking of atomic bonds in the cleavage plane. Owing to the competition between cleavage and dislocation emission, dislocation emission from the crack tip becomes easier when 6 at% Re is added to the Ni matrix. This means that Re is able to decrease the brittleness and improve the ductility of superalloys.

(3) γ_s and γ_s/γ_{us} for the $\{1\,0\,0\}$ plane increases with Re addition. Accordingly, dislocations more readily appear and the cleavage becomes more difficult. The value of γ_{us} can be changed by Re–Re atomic interaction. Ni–Re atomic interaction cannot decrease γ_{us}.

(4) In the MD simulation, the crack propagation velocity in the Ni matrix at 5 K observably decreases with Re addition. This means that Re–Ni atomic interaction can restrict the propagation velocity of cracks at low temperature.

(5) It is found that the velocity of a brittle crack is in inverse proportion to the adhesion work (W_{ad}). A small variation in W_{ad} results in a large change in crack velocity. Based on this result, the prediction that alloying elements with larger W_{ad} will hinder the propagation of brittle cracks may be made.

Acknowledgments

This work was supported by the National Basic Research Program of China (Grant No. 2011CB606402) and the National Natural Science Foundation of China (Grant No. 51071091).

References

[1] Jackson J J, Donachie M J, Henricks R J and Gell M 1977 *Metall. Trans.* A **8** 1615
[2] Gell M, Duhl D N and Giamei A F 1980 *Superalloys 1980* ed J K Tien *et al* (Metals Park, OH: ASM) p 205
[3] Kablov E N and Petrushin N V 2008 *Superalloys 2008* ed R C Reed *et al* (Warrendale, PA: TMS) p 901
[4] Yu J J, Hou G C, Zhao N R, Jin T, Sun X F, Guan H R and Hu Z Q 2006 *Rare Met. Mater. Eng.* **35** 1231–4
[5] Walston S, Cetel A, MacKay R, O'Hara1 K, Duhl D and Dreshfield R 2004 *Superalloys 2004* ed K A Green *et al* (Warrendale, PA: TMS) p 15
[6] Alessandro M, Finnis M W and Reed R C 2012 *Acta Mater.* **60** 2866–72
[7] Caron P and Khan T 1999 *Aerosp. Sci. Technol.* **3** 513–23
[8] Giamei A F and Anton D L 1985 *Metall. Mater. Trans.* A **16** 1997–2005
[9] Sato A, Harada H, Yokokawa T, Murakumo T, Koizumi Y, Kobayashi T and Imai H 2006 *Scr. Mater.* **54** 1679–84
[10] Zhang J X, Harada H, Rob Y, Koizumi Y and Kobayashi T 2008 *Acta Mater.* **56** 2975–87
[11] Schubert F, Rieck T and Ennis P J 2000 *Superalloys 2000* ed T M Pollock *et al* (Warrendale, PA: TMS) p 341–6
[12] Henderson M B and Martin J W 1996 *Acta. Mater.* **44** 111–26
[13] Ott M and Mughrabi H 1999 *Mater. Sci. Eng.* A **272** 24–30
[14] Hess B, Thijsse B J and Van der Giessen E 2005 *Phys. Rev.* B **71** 054111
[15] Xie H X, Wang C Y and Yu T 2008 *J. Mater. Res.* **23** 1597–03
[16] Xie H X, Wang C Y, Yu T and Du J P 2009 *Chin. Phys.* B **18** 251–8
[17] Guo Y F, Wang Y S, Wu W P and Zhao D L 2007 *Acta. Mater.* **55** 3891–7
[18] Gong X F, Yang G X, Fu Y H, Xie Y Q, Zhuang J and Ning X J 2009 *Comput. Mater. Sci.* **47** 320–5
[19] Chen K, Zhao L R and Tse J S 2004 *Mater. Sci. Eng.* A **365** 80–84
[20] Du J P, Wang C Y and Yu T 2013 *Modelling Simul. Mater. Sci. Eng.* **21** 015007
[21] Suo Z 1990 *Proc. R. Soc. Lond. Ser.* A **427** 331–58
[22] Reed R C, Yeh A C, Tin S, Babu S S and Miller M K 2004 *Scr. Mater.* **51** 327–31
[23] Srinivasan R, Banerjee R, Hwang J Y, Viswanathan G B, Tiley J, Dimiduk D M and Fraser H L 2009 *Phys. Rev. Lett.* **102** 086101
[24] Rice J 1988 *J. Appl. Mech.* **55** 98–103

[25] Allen M P and Tildesley D J 1987 *Computer Simulation of Liquids* (New York: Oxford University Press) p 83
[26] Riffkin J, Center for Simulation, University of Connecticut, CT, www.ims.uconn.edu/centers/simul/
[27] Mottura A, Miller M K and Reed R C 2008 *Superalloys 2008* ed R C Reed *et al* (Warrendale, PA: TMS) p 891
[28] Mottura A, Wu R T, Finnis M W and Reed R C 2008 *Acta. Mater.* **56** 2669–75
[29] Reed R C 2006 *The Superalloys Fundamentals and Applications* (New York: Cambridge University Press) p 55
[30] Rice J R 1992 *J. Mech. Phys. Solids* **40** 239
[31] Siegel D J 2005 *Appl. Phys. Lett.* **87** 121901
[32] Gordon Peter A and Neeraj T 2009 *Acta. Mater.* **57** 3091–100
[33] Rodary E, Rodney D, Proville L, Bréchet Y and Martin G 2004 *Phys. Rev.* B **70** 054111
[34] Finnis M W 1996 *J. Phys.: Condens. Matter.* **8** 5811–36
[35] Wang C and Wang C Y 2009 *Appl. Surf. Sci.* **255** 3669–75